Russian Geology and Geophysics © 2020, V.S. Sobolev IGM, Siberian Branch of the RAS
Vol. 61, No. 9, pp. 1036–1055, 2020 *DOI:10.15372/RGG2019144* *Geologiya i Geofizika*

Long-period ($10 < T < 20{,}000$ s) Magnetotelluric Studies in Northern Vietnam

V.M. Nikiforov†[a], I.M. Varentsov[b], G.N. Shkabarnya[a,✉], V.B. Kaplun[c], A.Yu. Zhukovin[a], Do Huy Cuong[d]

[a] *V.I. Il'ichev Pacific Oceanological Institute, Far Eastern Branch of the Russian Academy of Sciences, ul. Baltiiskaya 43, Vladivostok, 690041, Russia*

[b] *Schmidt Institute of Physics of the Earth, Russian Academy of Sciences, POB 30, Troitsk, 108840, Russia*

[c] *Yu.A. Kosygin Institute of Tectonics and Geophysics, Far Eastern Branch of the Russian Academy of Sciences, ul. Kim Yu Chena 65, Khabarovsk, 680000, Russia*

[d] *Institute of Marine Geology and Geophysics, Vietnam Academy of Science and Technology, Hanoi, Vietnam*

Received 7 February 2019; received in revised form 3 July 2019; accepted 28 August 2019

Abstract—We consider results of magnetotelluric and magnetovariational soundings in the period range $10 < T << 20\,000$ s in the North Vietnam area. The simple structure of magnetovariational responses is shown, which generally reflects the electrically conductive quasi-two-dimensional structure of the Earth's crust. Impedance responses form as a superposition of responses of local complex subsurface and quasi-two-dimensional regional deep-seated structures. Separation of local and regional effects made it possible to construct a geoelectrical depth model of the regional tectonosphere, whose main elements are electrically conductive subvertical trans-lithospheric faults and high-resistivity disturbances of the conductive asthenosphere. These elements, favoring the flow of telluric currents induced in deep-seated electrically conductive systems into the sedimentary cover, form zones of abnormal apparent-resistivity curves. The apparent resistivity monotonously increases with increasing the period up to 20,000 s. We called the combination of such elements of the geoelectrical model a ultradeep fluid–fault system (UDFFS). The modeling has established the location of three orthogonally intersecting UDFFS of NE and SE strikes in the North Vietnam area. It shows that conductive (fluid-saturated) translithospheric faults extending to the base of the sedimentary sequence control the location of petroleum fields and ore deposits. A method for separating local and regional magnetotelluric effects is proposed. It permits one to determine reliably the main strikes of a regional two-dimensional structure and the configuration of the apparent-resistivity curves along them.

Keywords: magnetotelluric sounding; tectonosphere; geoelectrical model; asthenosphere; deep fault; mantle fluid; petroleum field; Vietnam

INTRODUCTION

North Vietnam is located in the contact zone of tectonic plates whose age, degree of metamorphism, and type of magmatism vary. The main structure of the region is the basin of the Red River. It is believed that it results from a complex shift and lays on a continental base (Phuong, 1991; Phach, 2001). In the northern part, it overlaps the blocks of the China plate: the Yangtze Precambrian block stretching for more than 2000 km from Shanghai to the Red River and the Phanerozoic Bac Bo–Guangxi–Jiangxi Belt (Nielsen et al., 1999). In the south and southwest, it is blocked by the Phanerozoic Vietnam–Laos mobile Belt – an element of the Indochina Plate. The laying and development of the basin of the Red River occur under the influence of deep-seated faults of the northwestern direction. At sea, this basin is located across the axial line of the South China Sea. In the longitudinal direction of the basin, stepped thickness variation is observed. Based on the deep seismic sounding and gravity exploration data, the general nature of the structure of the Earth's crust is established. It varies from a continental thickness of 35–36 km in the northwest to a thinned continental thickness of 25–28 km in the southeast. Most researchers classify the basin of the Red River as a riftogenic structure. Insufficient knowledge of the deep-seated regional structure prevents one from solving fundamental and applied problems that influence the development of effective exploration directions (especially oil and gas exploration) and the rational use of natural resources in densely populated areas.

In 1996–1997, this gap was filled by Vietnamese and French researchers who performed a deep magnetotelluric sounding (MTS) along the profile (eight points) that crossed the Red River fault zone in the central part of the Hanoi basin (Doan et al., 2001). Later, Vietnamese scientists carried out an MTS using high-frequency equipment (Minh et al., 2011). It was shown by analyzing the data of those stud-

✉ Corresponding author.
E-mail address: shkabarnya@mail.ru (G.N. Shkabarnya)
† Deceased

ies that, in a high-frequency range (103–1 Hz, less often up to 0.1 Hz), the nature of electromagnetic field responses stably remained or naturally varied over the investigated area, and those interpretations generally reflected well the geoelectric structure of the upper part of the section under study. In a low-frequency range ($T > 10$ s), the stability of electromagnetic responses was lost. Interpreting those data led to conflicting results, which did not allow for the formation of a regularly changing deep-seated tectonic structure in the area under study.

The goal of this work is to estimate the effectiveness of magnetotelluric methods in a set of geological and geophysical studies, establish the features of electromagnetic processes in a low-frequency range in a complex geological and, accordingly, heterogeneous geoelectric medium, develop methods for separating local and regional magnetotelluric effects, and investigate the reflection of elements of a horizontally inhomogeneous geoelectric model in impedance and magnetic responses.

METHOD FOR RECORDING THE MT-FIELD COMPONENT VARIATIONS

Magnetotelluric research on the territory of North Vietnam as part of joint Russian–Vietnamese scientific cooperation programs in 2012–2013 and 2016–2017 were carried out at 20 points located along three profiles in the northeastern direction (Fig. 1). The MT field was recorded using a LEMI-025 three-component magnetometer (Korepanov et al., 2007) and a digital telluric field meter designed at the V.I. Il'ichev Pacific Oceanological Institute of the Far Eastern Branch of the Russian Academy of Sciences at points CBU, COT1, TRA, and BOR. At points COT2, NGV, and NIC, only horizontal electrical components were recorded. At the remaining points, the electric and magnetic components of the MT field were recorded using a LEMI-417 magnetotelluric station.

Before the beginning of each field season, the correspondence of real characteristics of the measuring equipment to their passport data was checked at the VLA magnetic observatory (Vladivostok, Russia). The length of the measuring electric lines was 400–700 m, which most often provided a signal level sufficient for reliable recording. However, at points located in the low-resistivity fault zones (HLG, YNB, TRS, PYN, and CBU), the signal level was comparable to noise, which affected the quality of their impedance estimates. The measuring electric lines were unwound in the North–South (x axis) and West–East (y axis) directions. At individual points, additional measuring lines were laid at an angle of 45° with respect to the main ones. The magnetic components at all points were recorded in a single system: the x axis is North–South, the y axis is West–East, and the z axis is vertically down.

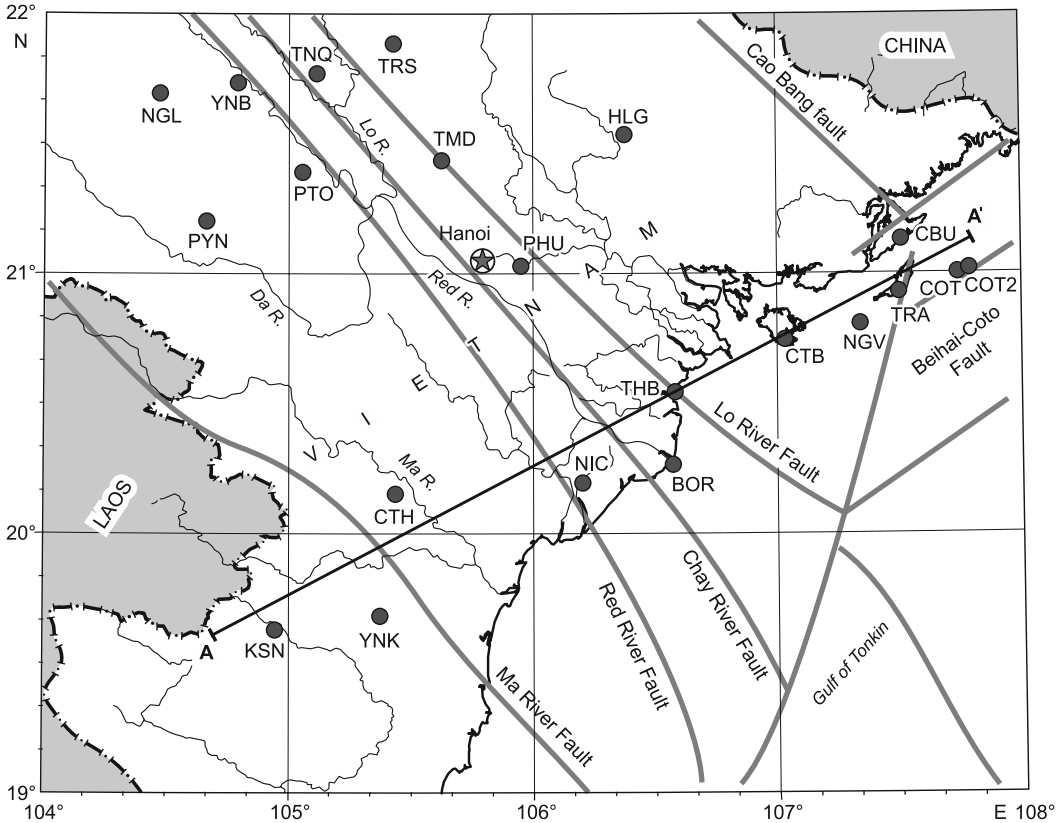

Fig. 1. Location of the MT-field observation points based on the Russian–Vietnamese programs in 2012–2017 and the main faults of North Vietnam. The solid line denotes the construction profile of the geoelectric section A–A′.

Due to complexity of the terrain and the wide development of stationary and semi-stationary electrical communication networks, it was not always possible to lay electrical measuring lines strictly in the azimuths of the axes selected, with deviations sometimes reaching 10°. These deviations were then taken into account during data processing. Among the unfavorable factors that reduced the recording quality of the MT field, one could observe that the measuring lines are regularly torn by the local population and that the natural potential (NP) course was gradient, especially at the terrain points with a large difference in altitude and a sharp change in the surface water under tropical rain conditions. The sampling frequency of magnetic and electrical variations was 1 Hz. The sampling times were synchronized with UTC by GPS. The duration of continuous recording sessions for the MT field ranged from 3 to 10 days, which provided an expanded range of processed periods from 15,000 to 20,000 s. All the MT field recording sessions were accompanied by synchronous recording of magnetic components at the PHU magnetic observatory (Hanoi) located in the center of the area studied.

MAGNETIC RESPONSE CHARACTERISTICS

Synchronous noise reduction processing of the data collected in 2012–2017 on the basis of closely located geomagnetic observatories is aimed at obtaining high-quality EM field transmission operators. Based on the general statements about a simpler structure of magnetovariational (MV) responses, the primary task is to obtain magnetic tippers (W) determined from a Wiese–Parkinson relation $H_z = [W] \cdot H_\tau$ and horizontal magnetic tensors $\left[M\left(r/r_b\right) \right]$, determined from relations $H_\tau(r) = \left[M\left(r/r_b\right) \right] \cdot H_\tau\left(r_b\right)$, in which H_τ is the horizontal magnetic field at a field point O(r) and a base point B(r_b).

At all points where magnetic field component variations were recorded, the source material supplemented by time series at four geomagnetic observatories (DLT and PHU – Vietnam, THJ and LZH – Southwest China) turned out to be quite suitable for obtaining MV responses.

Based on the data collected this way, the tipper and the horizontal magnetic tensor are estimated with respect to various base points using the multipoint processing of synchronous MT/MV data developed in the Institute of Physics of the Earth, Russian Academy of Sciences (Varentsov, 2002, 2016; Varentsov et al., 2003; Varentsov, 2015). At all sounding points, including the PHU magnetic observatory, stable multi-RRMC estimates for the tipper are obtained (Varentsov, 2015) using from two to four remote points.

For periods from 256 to 8192 s, the maps of the real Wiese–Parkinson tippers on the area under study are constructed (Fig. 2). In its northeastern part, including the PHU observatory, these vectors are consistently directed northeastward in the entire presented period range (the arrows are directed away from the conductor). In the southwestern part of the area at points KSN, YNK, and CTH, the arrows of the induction vectors have diametrically opposite directions. At points NGL, YNB, and PYN, which are located in the northwest of the area, the induction vectors are characterized by a low level of modulus, and their directions cannot be determined accurately. The results of calculating the tippers allow one to distinguish a strip that denotes the redirection of induction vectors, which stretches for more than 300 km through the entire area under study from northwest to southeast.

The primary horizontal tensors are determined relative to the PHU observatory. The quality of the received horizontal responses at all points is uniformly high. However, judging by the nature of the tippers (Fig. 2), the PHU observatory is located in the gradient zone of the anomalous magnetic field associated with a deep-seated electrically conductive body. In this regard, the horizontal MV responses estimated with respect to PHU are recalculated (Varentsov, 2015) relative to the sounding points that are the farthest from the identified anomalies. Figure 3 shows two versions of the horizontal magnetic response map: the one relative to CTB (Cat Ba Island) and the one relative to HLG (100 km northeast of Hanoi).

Graphically, magnetic responses are represented as ellipses of magnetic tensors. For clarity, the ellipses are rotated at an angle of 90° so that their long axes emphasize the direction of the strike of electrically conductive objects in the lower half-space. When comparing Figs. 3*a* and 3b, one can see that, if the base point changes from CTB to HLG, there is no fundamental restructuring of the anomalous field of horizontal magnetic responses. Recalculation with respect to point HLG seems to be optimal in accuracy and simplicity in terms of the spatial structure of horizontal MV responses. In this recalculation, for all periods over 256 s, the isolines of the maximum values of the horizontal MV responses describe a slightly complicated trapezoidal structure of the southwestern strike. Due to the lack of field observations in the western part of the area, the southwestern wing of the anomalous structure has been studied only partially. The region of minimum tipper values is located inside the region of maximum values of the horizontal MV responses. This behavior of anomalous vertical and horizontal fields obviously indicates that the electrical structure of the lower half-space is simple and close to a two-dimensional structure and that it creates the above-mentioned anomalies. This is also indicated by the nature of the ellipses of horizontal magnetic tensors, characterized by a large predominance of long axes over short ones.

CHARACTERISTICS OF MAGNETOTELLURIC RESPONSES

Impedance estimates at different points are quite diverse in quality. Stable multi-RRMC impedance estimates (Varentsov, 2002, 2016; Varentsov et al., 2003) with the use of

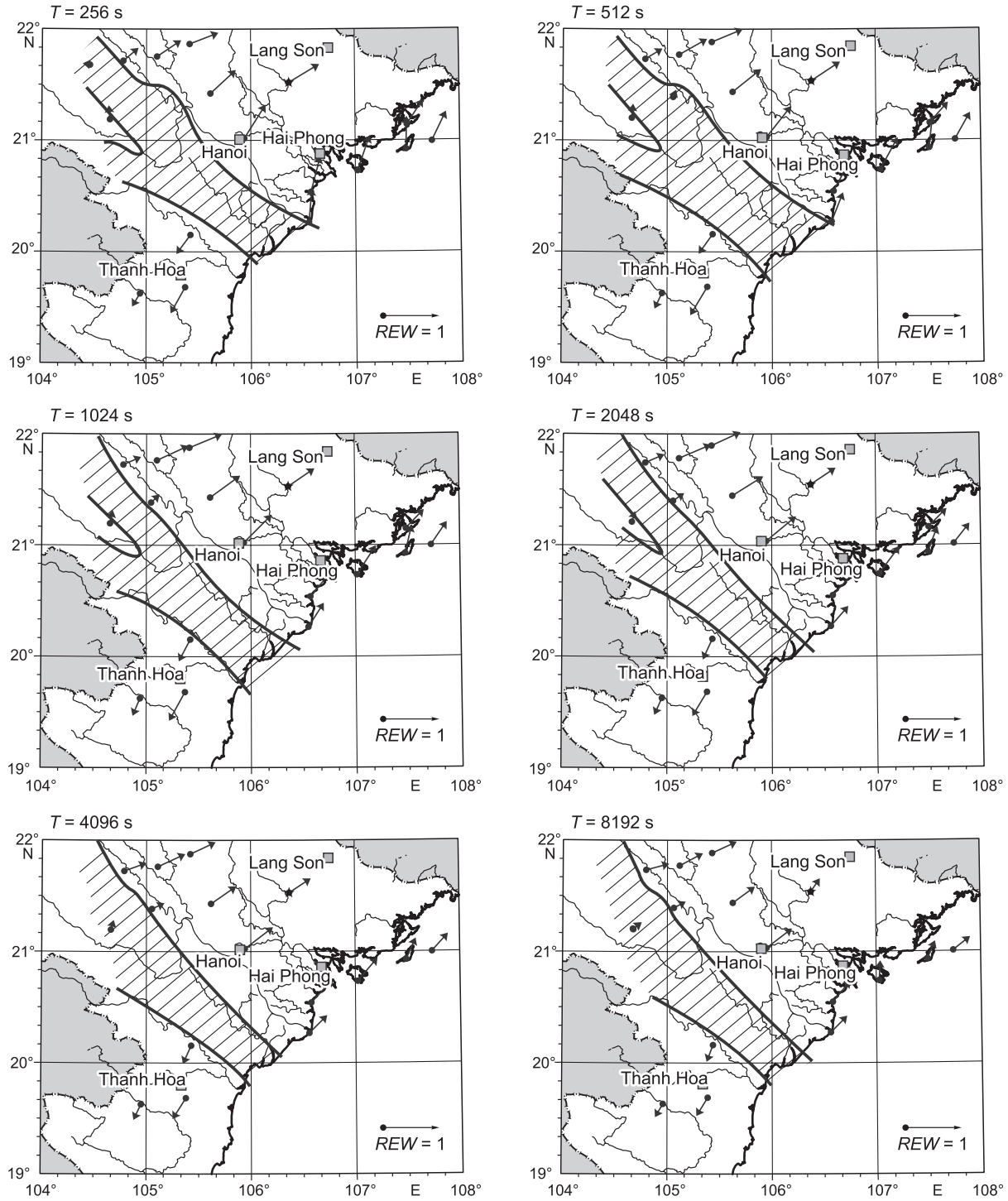

Fig. 2. Real induction vectors at the observation points of magnetic field components. Hatching indicates the zones where induction vectors change directions. The lower right part of the maps shows the value of the unit vector *REW*.

two to four remote points could be obtained only in individual cases. The extreme invariant parameters of apparent resistivities and phases in many cases are very different, which makes it impossible to establish tendencies in their changes on the territory under study. Effective apparent resistivities and phases match only at individual points: PTO, KSN, YNK, NGL, and YNB. The MT field processing results meant for determining the tensor components of the impedance relating the electrical and magnetic fields by an expression $E_\tau = [Z] \cdot H_\tau$ lead one to the same conclusion as the results previously obtained in this area by Vietnamese and French researchers (Doan et al., 2001): the interpreta-

a

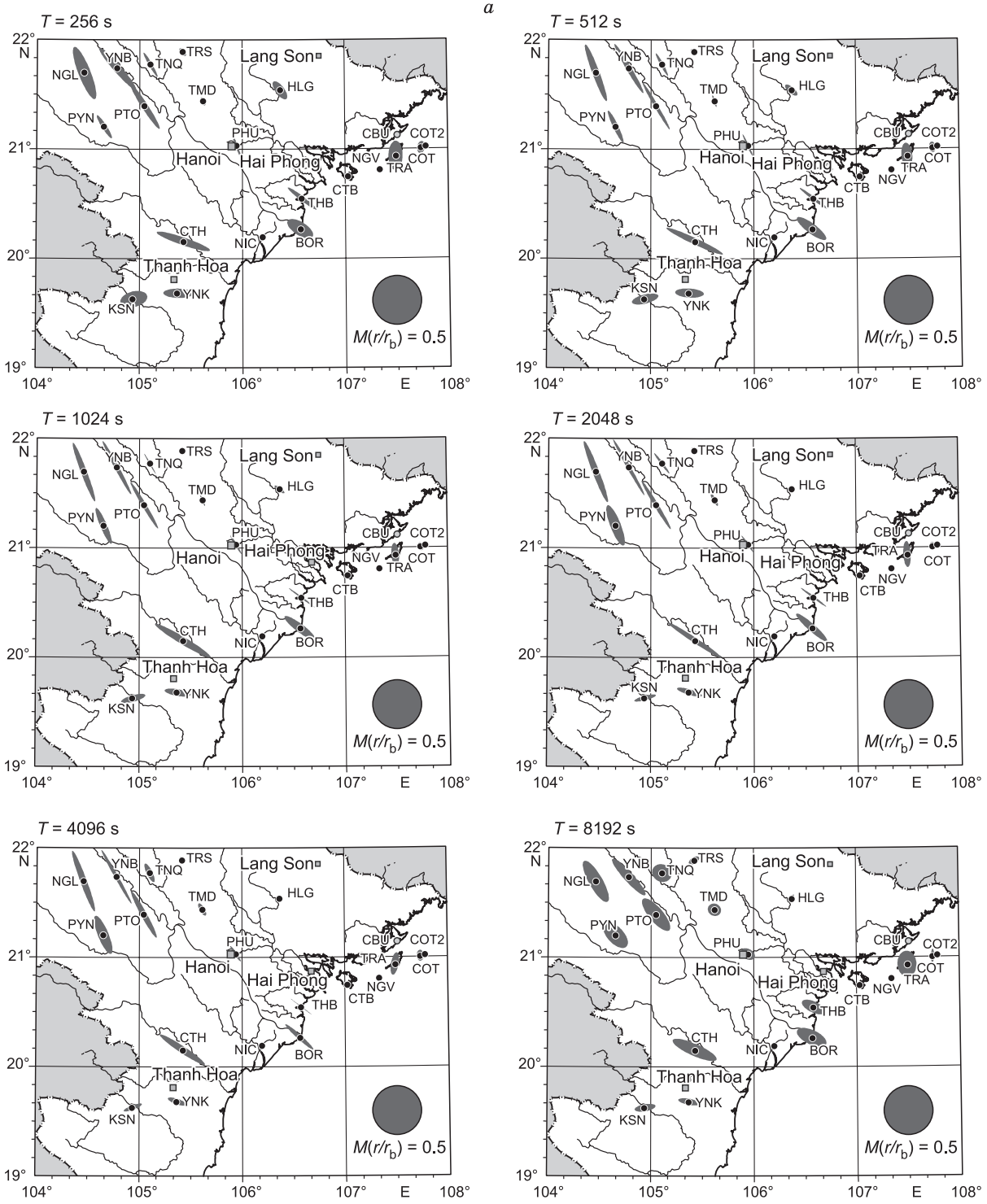

continued to next page

tion of magnetotelluric responses of varying area inevitably leads to conflicting geological constructions (Dinh et al., 2018) where each MTS point is identified with a separate geoelectric block, which strongly differs from the neighboring ones with respect to electrical resistivity.

The geological structure of North Vietnam, the tectonics, and, as shown above, the vertical and horizontal magnetic responses of the MT field indicate that the presence of regional two-dimensional or quasi-two-dimensional geoelectric structures is highly probable. At the same time, judging

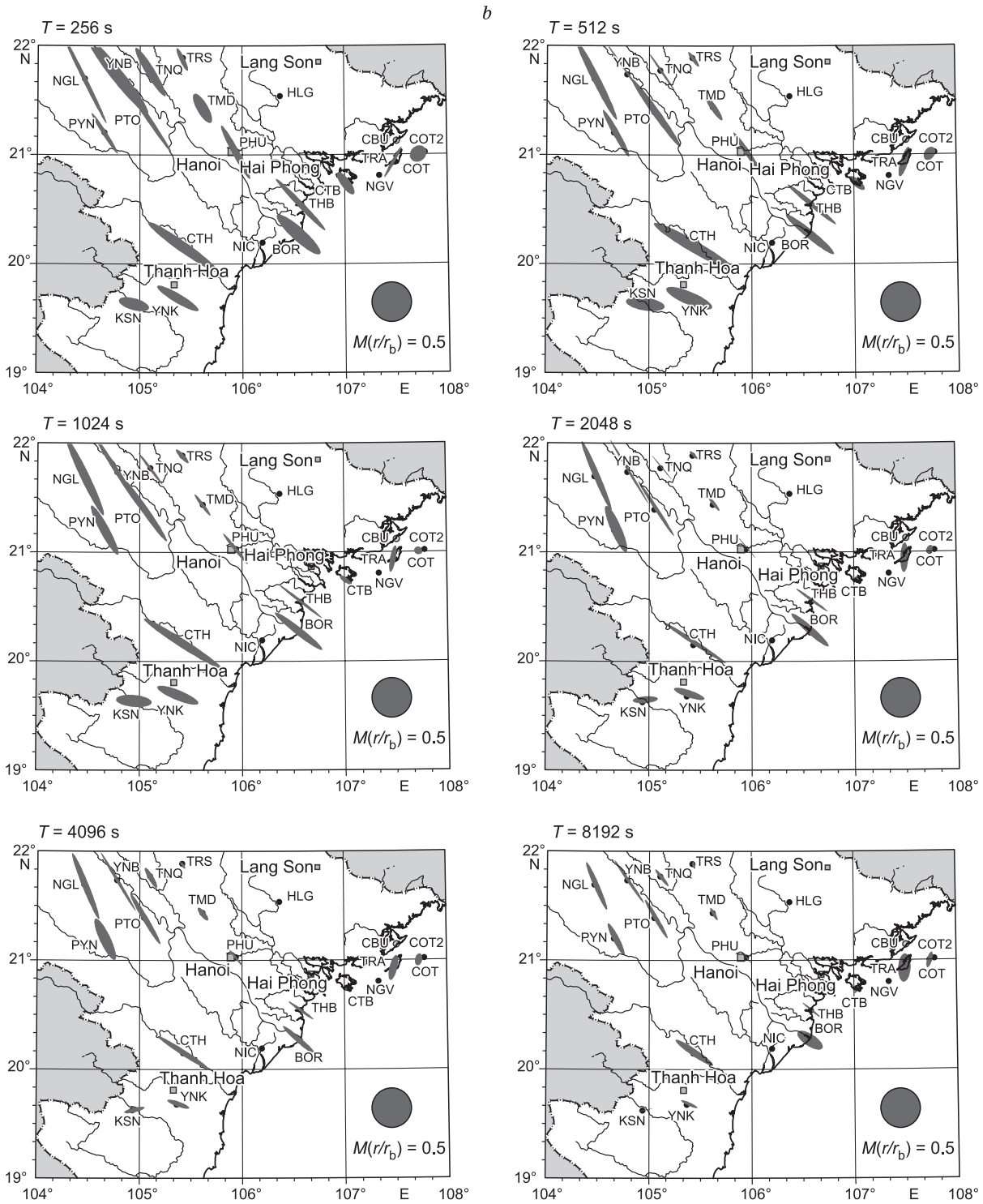

Fig. 3. Maps of the horizontal magnetic responses. *a*, Base point CTB, *b*, base point HLG: the ellipses of the horizontal magnetic responses are rotated at an angle of 90°. The lower right part of the maps shows the scale M(r/r_b).

by the available data, sharp inhomogeneities in the electrical resistivity of near-surface local structures (discontinuities, surface and underground waters, etc.) complicate the dependence between electric and magnetic fields, which is a response to the superposition of deep-seated and surface structures. According to (Berdichevskii and Dmitriev, 2010), the local-regional impedance of structural superposition has the form

$$(Z^S) = (e)\times(Z^R), \quad (1)$$

where (Z^S) is the local-regional impedance calculated from the MT field recordings, (Z^R) is the regional impedance, and (e) is the local electrical distortion tensor.

The studies of impedance (Z^S) in North Vietnam reveal a strong displacement of dispersion relations of the second kind. According to (Berdichevskii and Dmitriev, 2010), "if three-dimensional near-surface inhomogeneities form geological noise that violates the dispersion relation of the second kind, then various geological structures are obtained as a result of the inversion of apparent resistivities and impedance phases". This phenomenon can be eliminated by separating the regional and local effects summarized in the values of (Z^S).

The ability to detect and account for distortions created by local near-surface heterogeneities has been studied by many researchers and described in numerous publications. Currently, the Bahr (Bahr, 1988) and Groom–Bailey (Groom and Bailey, 1989) methods are widely used in practice the most. The phase tensor analysis is especially popular (Caldwell et al., 2004). But, as shown by MTS in folded areas (the mountainous regions of Sakhalin, Sikhote-Alin, and Vietnam), where near-surface formations usually have high resistivity and are dissected into different-scale units by low-resistivity displacements, the above-given methods cannot ensure stable values, which leads to conflicting geological constructions. Apparently, the reason is that, in all the methods used, the main directions and the main values of the regional impedance tensor are determined as combinations of eight calculated impedance tensor components in the coordinate system of observation of electric and magnetic fields. Each of these components, calculated against the background of geological and industrial noise, introduces a certain error, and then these errors add up. To minimize this drawback, we propose a more laborious method that ensures a result stable for this area, which is known as the azimuthal analysis of apparent resistivity (Nikiforov et al., 2016). As is known (Berdichevskii and Dmitriev, 2010), if the x and y axes are directed along and across a regional two-dimensional structure, then Eq. (1) takes the form

$$\left[Z^S\right] = \begin{bmatrix} Z^S_{xx} & Z^S_{xy} \\ Z^S_{yx} & Z^S_{yy} \end{bmatrix} = \begin{bmatrix} e_{xx} & e_{xy} \\ e_{yx} & e_{yy} \end{bmatrix} \cdot \begin{bmatrix} 0 & \zeta_1^R \\ \zeta_2^R & 0 \end{bmatrix} = \begin{bmatrix} -e_{xy}\zeta_2^R & e_{xx}\zeta_1^R \\ -e_{yy}\zeta_2^R & e_{yx}\zeta_1^R \end{bmatrix}, \quad (2)$$

where ζ_1^R and ζ_2^R are the main values of the two-dimensional regional tensor, and e_{xx}, e_{xy}, e_{yx}, and e_{yy} denote the real local electric distortion tensor components.

Let there be electric lines laid in the North–South (N) and West–East (W) directions. Electric fields recorded by these lines are expressed via components in the coordinate system x, y as follows:

$$E_N = a_{Nx}\cdot E_x + a_{Ny}\cdot E_y, \quad (3)$$

$$E_W = a_{Wx}\cdot E_x + a_{Wy}\cdot E_y. \quad (4)$$

Here a_{Nx}, a_{Ny}, a_{Wx}, and a_{Wy} denote the real coefficients projecting the values of E_x and E_y onto the North–South and West–East directions. Uniting expressions (3) and (4) with Eq. (2), we obtain:

$$E_N = \left(-a_{Nx}\cdot e_{xy} - a_{Ny}\cdot e_{yy}\right)\cdot\zeta_2^R\cdot H_x + \left(a_{Nx}\cdot e_{xx} + a_{Ny}\cdot e_{yx}\right)\cdot\zeta_1^R\cdot H_y, \quad (5)$$

$$E_W = \left(-a_{Wx}\cdot e_{xy} - a_{Wy}\cdot e_{yy}\right)\cdot\zeta_2^R\cdot H_x + \left(a_{Wx}\cdot e_{xx} + a_{Wy}\cdot e_{yx}\right)\cdot\zeta_1^R\cdot H_y\sum_{i=1}^{n} X_i^2. \quad (6)$$

As combinations of real frequency-independent numbers are enclosed in parentheses, they can be replaced by some indefinite coefficients:

$$-a_{Nx}\cdot e_{xy} - a_{Ny}\cdot e_{yy} = C_1, \quad (7)$$

$$a_{Nx}\cdot e_{xx} + a_{Ny}\cdot e_{yx} = C_2, \quad (8)$$

$$-a_{Wx}\cdot e_{xy} - a_{Wy}\cdot e_{yy} = C_3, \quad (9)$$

$$a_{Wx}\cdot e_{xx} + a_{Wy}\cdot e_{yx} = C_4. \quad (10)$$

This replacement makes Eqs. (5) and (6) quite simple:

$$E_N = C_1\cdot\zeta_2^R\cdot H_x + C_2\cdot\zeta_1^R\cdot H_y, \quad (11)$$

$$E_W = C_3\cdot\zeta_2^R\cdot H_x + C_4\cdot\zeta_1^R\cdot H_y. \quad (12)$$

As can be seen from Eqs. (11) and (12), the electric fields measured in the lines laid in the North–South and West–East directions are related to the magnetic field components along and across the two-dimensional regional structure of the same type through the main values of the impedance tensor. The action of local heterogeneity in this case comes down to changing the scale of the main values of the regional impedance tensor, which is expressed in bilogarithmic coordinates as a conformal shift of the curves.

The solutions of Eqs. (11) and (12) in a wide period range yield pairs of conformal curves $C_1\cdot\zeta_2^R(T)$, $C_3\cdot\zeta_2^R(T)$ and $C_2\cdot\zeta_1^R(T)$, $C_4\cdot\zeta_1^R(T)$, shifted relative to true values by the values of undetermined coefficients C_1, C_2 and C_3, C_4. Their role is similar to that of frequency-independent factors determining the intensity of static distortions typical of all methods of local-regional expansions (Berdichevskii et al., 1991; Kuznetsov, 2005; Berdichevskii and Dmitriev, 2010).

Technically, the separation of local and regional effects is carried out by incrementally (usually starting from the South–North direction and then by a step of 10°) increasing the angle of rotation of the coordinate system xy, into which the horizontal magnetic field components H_x and H_y, initially recorded in the South–North and West–East directions,

are converted. Then, in a wide period range, coefficients $Z_{Nx}(T)$, $Z_{Wx}(T)$, $Z_{Ny}(T)$, and $Z_{Wy}(T)$, which relate the electric field in the South–North and West–East directions with the horizontal components H_x and H_y are calculated:

$$E_N = Z_{Nx} \cdot H_x + Z_{Ny} \cdot H_y , \quad (13)$$

$$E_W = Z_{Wx} \cdot H_x + Z_{Wy} \cdot H_y . \quad (14)$$

Reaching the conformity of curves in pairs $\left|Z_{Nx}(T)\right|$ and $\left|Z_{Wx}(T)\right|$; $\left|Z_{Ny}(T)\right|$ and $\left|Z_{Wy}(T)\right|$ ends the process of increasing the angle of rotation of the coordinate system *xy*. According to Eqs. (11) and (12), this angle defines the main directions of the regional impedance tensor. In this case, the main values of the impedance tensor are

$$C_1 \cdot \zeta_2^R = Z_{Nx}(T); C_3 \cdot \zeta_2^R = Z_{Wx}(T) , \quad (15)$$

$$C_2 \cdot \zeta_1^R = Z_{Ny}(T); C_4 \cdot \zeta_1^R = Z_{Wy}(T) . \quad (16)$$

It should be noted that, if the observation point has an additional electrical measuring line laid in direction α, then it can be used to similarly obtain coefficients $Z_{\alpha x}(T)$ and $Z_{\alpha y}(T)$, which possess the above-described properties. Therefore, the use of additional lines for recording the MT field allows one to control the reliability of determining the principal values of the regional impedance tensor.

The values of $Z_{Nx}(T)$, $Z_{Wx}(T)$, $Z_{Ny}(T)$, and $Z_{Wy}(T)$ are used to calculate the apparent resistivity curves $\rho_{Nx}(T)$, $\rho_{Wx}(T)$, $\rho_{Ny}(T)$, and $\rho_{Wy}(T)$, on which the shape details can be seen more clearly. Figure 4 shows an example of apparent resistivity curves calculated using the method discussed above. As seen from the figure, with the position of the axes $x \sim 335°$ and $y \sim 65°$, the apparent resistivity forms two conformal groups $\rho_{\alpha x}(T)$, $\rho_{Nx}(T)$, $\rho_{Wx}(T)$ and $\rho_{\alpha y}(T)$, $\rho_{Ny}(T)$, $\rho_{Wy}(T)$. Such division into two polarizations indicates that there really is a regional structure close to a two-dimensional one. The main impedance values are determined with an accuracy to an indefinite constant factor. Given this circumstance, below we consider curves $\rho^*_{xy} = \sqrt{\rho_{Ny} \cdot \rho_{Wy}}$ and $\rho^*_{yx} = \sqrt{\rho_{Nx} \cdot \rho_{Wx}}$, which are also shifted relative to their true position. The fact of mismatch between the estimated value and the true value is denoted by * above ρ.

Figure 5 shows the apparent resistivity curves calculated by the method considered above or by the method of rotation of the impedance tensor with further verification of the conformity conditions (13) and (14). On the territory of North Vietnam, two main directions are reliably distinguished at almost all points: the first corresponds to the direction of the *x* axis 325–335°, and the second corresponds to the direction of the *y* axis 55–65°. Only at point TRS, which is located in a crushing zone and, accordingly, in a zone of strong surface distortions, ρ^*_{xy} and ρ^*_{yx} could not be obtained.

Apparent resistivity in the territory of North Vietnam is distinguished by its behavior in a long-period range $T > 500$ s. Figure 5*a* shows a family of curves ρ^*_{xy}, represented in general terms by conformal individual curves. These curves in an interval of periods of $10 < T < 100$ have an ascending branch further replaced by a maximum and a stable descending branch, which in some cases continues until $T = 10{,}000$ s. Similarly, in a long-period interval, there is family ρ^*_{yx} (Fig. 5*b*). The difference lies in the variety of shapes in short periods. However, despite the large scatter in the levels of individual curves in both families, the geometric mean curves ρ^{*m}_{yx} and ρ^{*m}_{xy} are both fairly close in level and conformal at $T > 500$ s. Formally, the mutually perpendicular curves ρ^{*m}_{yx} and ρ^{*m}_{xy} also indicate the presence of a layered background deep-seated geoelectric section, in which the electrical resistivity decreases with depth starting from a certain boundary.

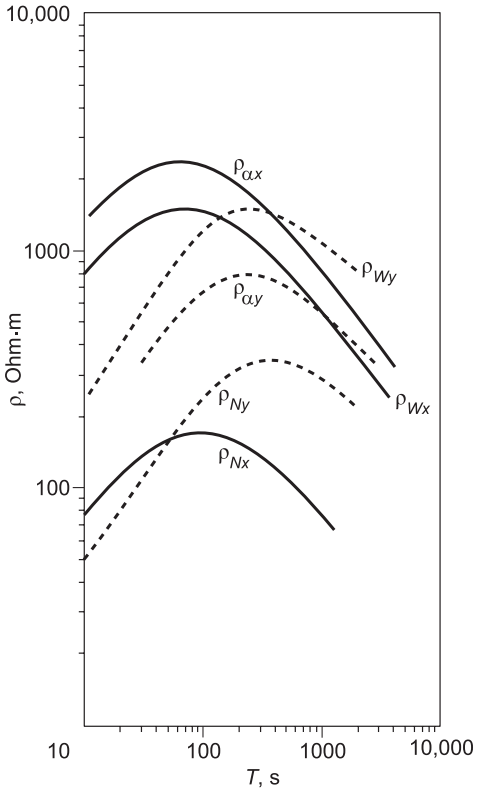

Fig. 4. Examples of the apparent resistivity curves calculated at COT according to electric field variations in the North-West (*N*), West-East (*W*), and North-West–South-East (*NW-SE* = 135°) lines, as well as to magnetic variations in the main impedance tensor directions *X* and *Y*. The dotted lines denote the direction of the *x* axis, which is 335°, and the solid lines denote the direction of the *y* axis, which is 65°.

Other features of the deep-seated geoelectric section are obtained from the curves presented in Fig. 5*c*, *d*. Both families, one of which is formed by individual curves ρ_{xy} (Fig. 5*c*) and the other one by individual curves ρ^*_{yx} (Fig. 5*d*), are very similar to each other. In a period range $10 < T < 1000$ s, the individual curves ρ^*_{xy} and ρ^*_{yx} have asymptotically ascending branches (at points NIC, HLG, KSN, THB, BOR, CTH, and CTB), sometimes complicated by bends (ρ^*_{xy} and ρ^*_{yx} at point CTH and ρ^*_{yx} at points THB and HLG). In most cases, there

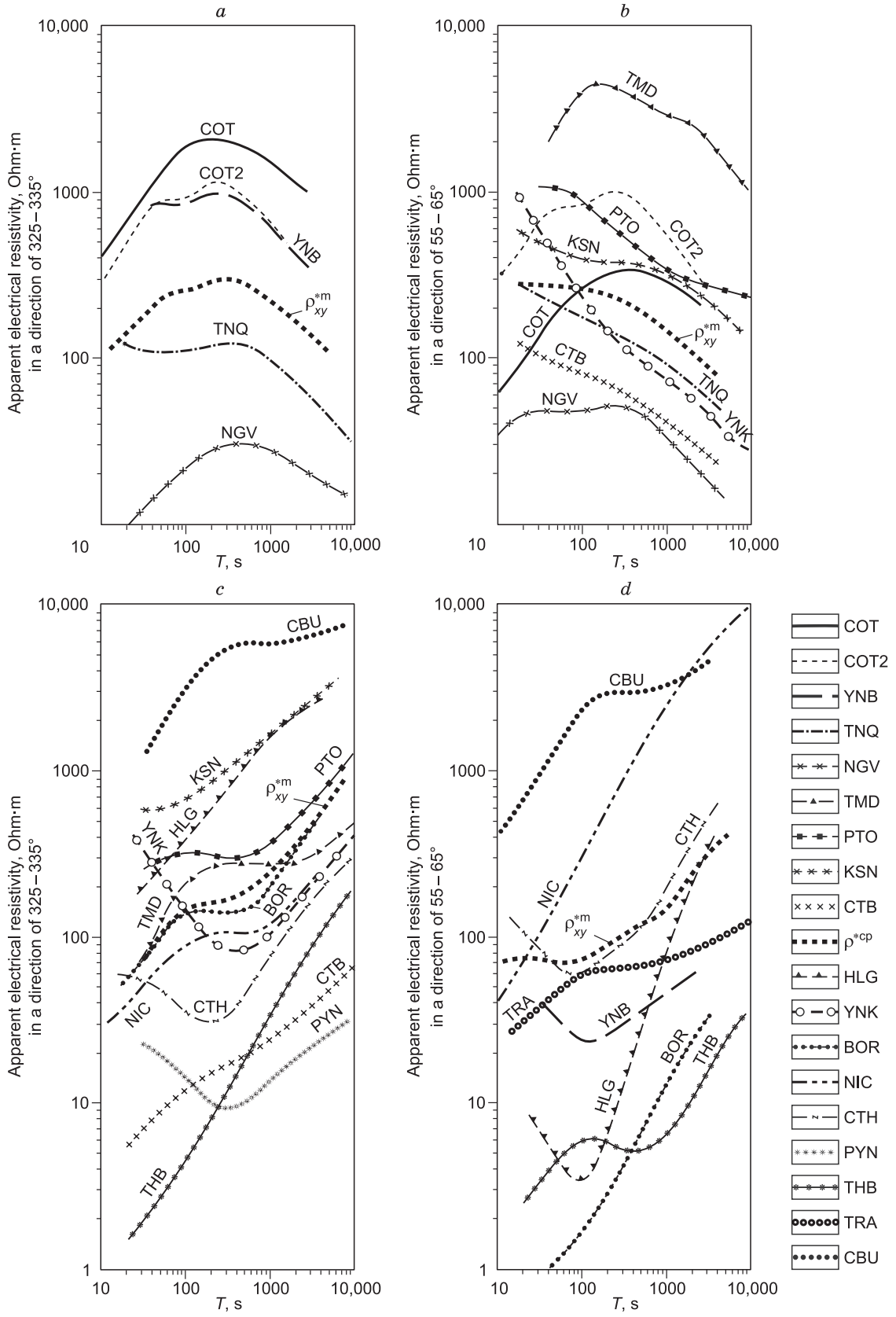

Fig. 5. Magnetotelluric sounding curves. *a*, *c*, MTS curves in a direction of 325–335° (ρ_{xy}); *b*, *d*, MTS curves in a direction of 55–65° (ρ_{yx}). The reference designations have lines types for the MTS points denoted in Fig. 1. ρ_{xy}^{m} and ρ_{yx}^{m} are the geometric mean MTS in groups.

is a minimum on the curves in this range, and the position of this minimum on the axis of periods varies from point to point. All the curves of both families, regardless of their individual shape in a short-period interval, have a steep ascending branch at $T > 1000$ s, which at some points is traced to $T = 20{,}000$ s. It is noteworthy that, despite the very large scatter in the apparent resistivity levels of individual curves, which is three to four orders of magnitude, geometric averaging yields the values of ρ^{*m}_{xy} and ρ^{*m}_{yx}, which are similar in shape and level (Fig. 5). This kind of curves can theoretically correspond to a plane-layered geoelectric section underlain by an absolute insulator of infinite power.

CONSTRUCTION OF A GEOELECTRIC MODEL OF TECTONOSPHERE OF THE FIRST APPROXIMATION

It is revealed by analyzing the MT and MV responses of the medium in Northern Vietnam that the anomalous vertical and anomalous horizontal fields have a relatively simple structure, which basically corresponds to the two-dimensional geoelectric structures of the lower half-space. The structure of the electric response field turns out to be more complicated, although it should be noted as a positive factor that the southeast direction of the domain of anomalous values of the vertical and horizontal magnetic fields corresponds to one of the main directions of the regional impedance tensor.

It is shown by regionalizing curves ρ^{*}_{xy} and ρ^{*}_{yx} that, on the relatively small territory of North Vietnam, in both main directions, the apparent resistivity curves in their long-period parts transform from descending to asymptotically ascending. Explaining the nature of ascending branches is crucial for describing the geoelectric model of tectonosphere. In the coastal zone, an abnormal increase in apparent resistivity is usually associated with the "coastal" effect (Moroz, 1991; Nikiforov et al., 2004; Utada and Baba, 2014). However, North Vietnam is washed by the shallow Gulf of Tonkin (a 100-m isobath is located more than 400 km from the coastline of the area under study), which does not allow one to relate the anomalous effect with the influence of the sea. Another convincing and fundamentally new circumstance that excludes the effect of the "coastal" effect is the fact that the anomalous behavior of the apparent resistivity curves is observed in three zones of different strikes: one of them stretches along the coast in a northeastern direction, and the other two orthogonally cross the former in a southeastern direction. Inside these zones, abnormally ascending branches are observed across the curves with respect to the zone strike (on curves ρ^{*}_{xy} in the zone of northeastern strike and on the curves ρ^{*}_{yx} in the zones of southeastern strike), which can be traced to periods of 10,000–15,000 s.

It can be noted that extended ascending branches on apparent resistivity curves are also often observed in continental structures, for example, within kimberlite-containing areas (Pospeeva, 2008).

The nature of anomalous MV and MT responses is probably related with the specific features of layer-block structure of tectonosphere, in which vertical (steep-dip) interfaces contribute to the formation of vertical electrical currents transforming into horizontal currents near the day surface. Based on the assumption that the effective apparent resistivities agree with each other in the regions where horizontal currents are minimal, MTS at these points can be used to obtain a general idea about the layered geoelectric section of tectonosphere. The data at points PTO, KSN, YNK, NGL, and YNB, which satisfy this condition, serve as a basis for developing the layered background model of the tectonosphere of North Vietnam.

For the above-given points, 1D inversion is performed (Varentsov et al., 2003). On graph $\rho(H)$, the results of this inversion form a relatively wide range of possible values of electrical resistivity, which regularly changes over depth (Fig. 6). The bounds of maximum and minimum values of this domain are practically conformal, favoring the separation of individual geoelectric horizons of the tectonosphere. Graph $\rho(H)$ in a depth interval of 200–500 km virtually matches the standard geoelectric section (Van'yan et al., 1986; Van'yan, 1997), which validates the confidence in its upper part (0–200 km). In this depth interval, the following geoelectric horizons can be distinguished (Table 1).

Analyzing the ratio of inverted electrical resistivity reveals two different tiers of the geoelectric section of the tectonosphere of North Vietnam. The upper tier, which occupies a depth interval of 0–50 km, is characterized by a significant (two to three orders of magnitude) underestimation of the inverted electrical resistivity relative to the standard. Most reference observation points contain low-resistivity (10–20 Ohm·m) formations in an interval of depths

Table 1. Geoelectric horizons of the tectonosphere model of North Vietnam

No.	Names of geoelectric horizons	Roof depth, km	Base depth, km	Range of resistivity, Ohm·m
1	Sedimentary cover	0	1–2	60–300
2	Upper part of the consolidated crust	0–2	10–20	200–1000
3	Lower part of the Earth's crust	10–20	30–50	15–30
4	Subcrustal lithosphere	30–50	120–150	1000–10000
5	Asthenosphere	120–150		50–100
6	Standard (gradient) geoelectric section (Van'yan, 1997)			

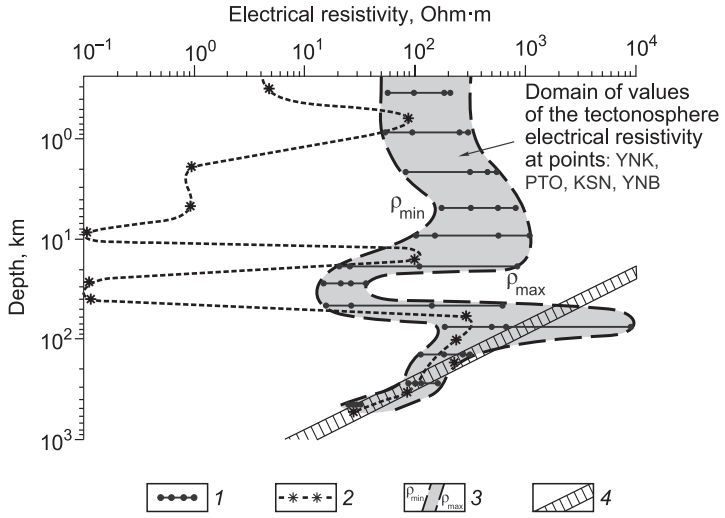

Fig. 6. Summary chart of the distribution of electrical resistivity of the tectonospheric rocks of North Vietnam (according to the efficient apparent resistivity inversion data). *1*, resistivity inversion at points YNK, PTO, KSN, and YNB; *2*, resistivity inversion at point NGL; *3*, boundaries of the domain of possible values of the electrical resistivity in the tectonosphere of North Vietnam; *4*, standard (Van'yan, 1997) resistivity of the tectonosphere rocks.

from 10 to 50 km. Some points located within fault zones, such as point NGL, have very low resistivities (1–10 Ohm·m) in a depth interval from 0 to 10 km. However, starting from 30 km and deeper, the inverted resistivity distribution is the same as at all other strong points. This fact can be interpreted as a manifestation of low-resistivity fault zones extending to a depth of 10–15 km.

The lower tier of the geoelectric section, studied in a depth interval of 50–450 km, is characterized by a small deviation of the inverted resistivity from the standard. A certain underestimation of inverted resistivities is observed only in a range of 120–250 km, which can be related to the presence of electrically conductive (50–100 Ohm·m) layers of the asthenosphere in the section of the tectonosphere.

When it comes to searching for a class of inhomogeneities located in the above-mentioned layered geoelectric section, which could be represented as ascending branches up to periods higher than 10,000 s on the apparent resistivity curves, a special attention is paid to a model (Nikiforov et al., 2014, 2018) referred to as a ultradeep fluid-fault system (UDFFS). This UDFFS is comprised of three main elements. The first one is a low-resistivity body in the form of a vertical stratum developed in lithosphere and under its bottom, and this body violates the continuity of electrical conductivity of asthenosphere. On both sides of it in the lithosphere, there are subvertical (steeply dipping) electrically conductive relatively thin layers that divide the lithosphere into separate geoblocks. These strata, identified with the fluid-saturated crushing zones of deep-seated faults, provide a galvanic coupling between the sublithospheric conductive horizons and the conductive layers of the sedimentary cover. This coupling ensures an electric circuit through which the current, which is induced in the sublithospheric horizons and enriched with long-period components, enters the sedimentary stratum. In the region between the outputs of the conductive faults to the surface, this additional current transforms the frequency response of the medium.

The transformation of the frequency characteristics of responses (and, accordingly, the apparent resistivity) depending on the details of the model of the block-layered tectonosphere of North Vietnam are studied in a two-dimensional version (Fig. 7). The figure shows the simulation results for profile DD′ passing in the northwestern direction through the MTS points NGV, CTB, TMD, and TRS. The UDFFS system is placed into a layered-block geoelectric section with its parameters given in the table. Its 40-km wide high-resistivity element with an electrical resistivity $\rho_{в}$ = 1000 Ohm·m divides the electrically conductive asthenosphere ($\rho_{ast.}$ = 20 Ohm·m) into electrically insulated parts. Vertical conductive layers ($\rho_{ins.}$ = 5 Ohm·m) with a thickness of 2 km, which simulate the fluid-saturated zones of deep-seated faults, are placed into the high-resistivity lithosphere ($\rho_{lit.}$ = 1000 Ohm·m). The upper part of the section is a layer reflecting the sedimentary sequence of variable thickness (up to 3 km) and resistivity ($\rho_{sed.}$ = 10–100 Ohm·m). At the central part of the model corresponding to the Hanoi depression, the resistivity of the sedimentary stratum is 10 Ohm·m. The UDFFS in the section creates an anomalous effect on the transverse apparent resistivity curves in the form of pulling in of their ascending branches, which is clearly demonstrated by the calculation results for models *A* and *B*, differing only in the values of the electrical resistivity of the conductive plate ($\rho_{cru.}$) in the Earth's crust in a depth interval of 15–25 km. If $\rho_{cru.}$= 100 Ohm·m and larger, the ascending branch $\rho^{\perp}$ at all points on the profile section between the faults monotonically increases in a pe-

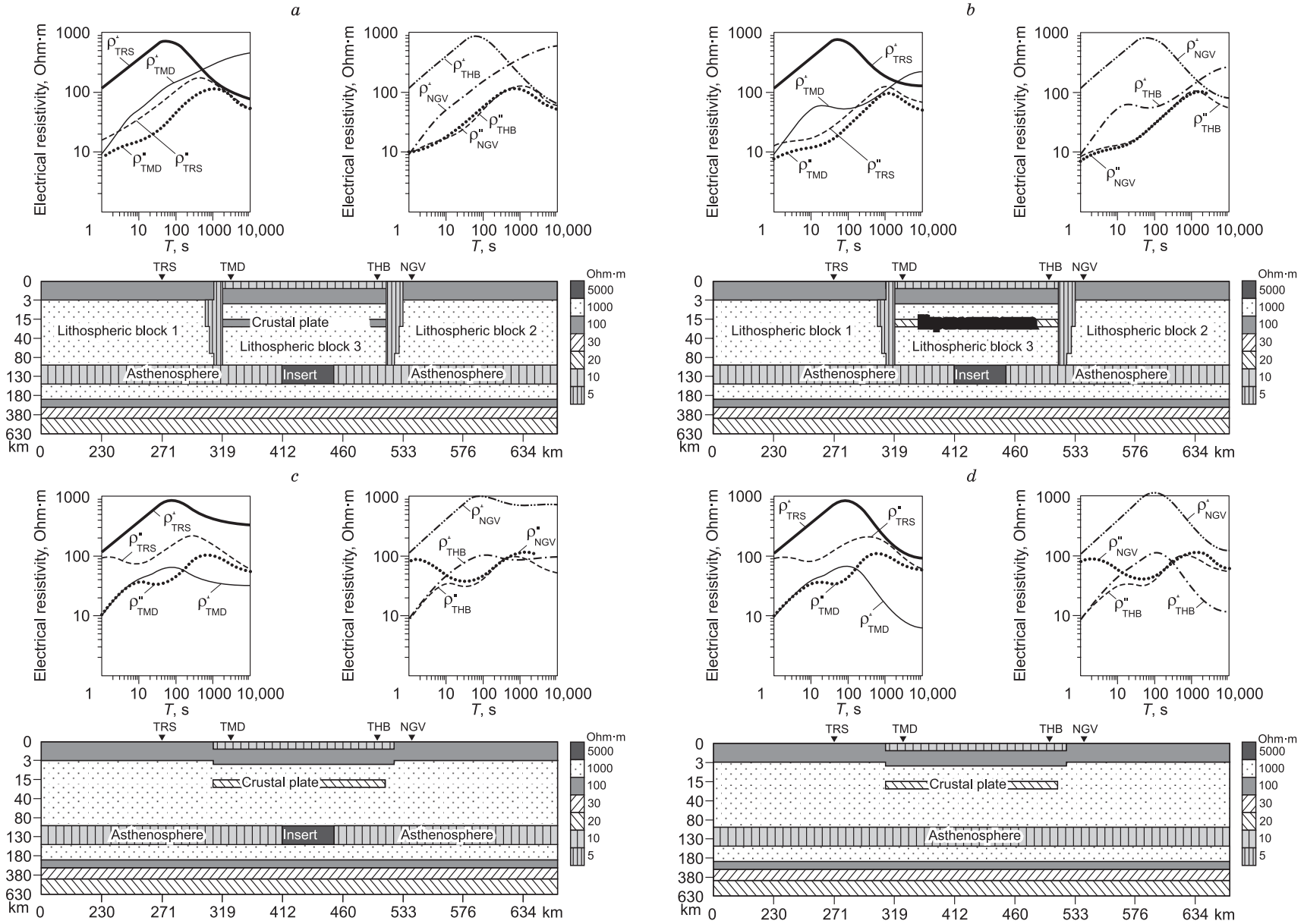

Fig. 7. Theoretical MTS curves different versions of the block-layered model of the tectonosphere. *a*, UDFFS with a conductive layer in the Earth's crust (15–25 km) $\rho_к$ = 180 Ohm·m; *b*, UDFFS (15–25 km) $\rho_к$ = 20 Ohm·m; *c*, UDFFS with a conductive layer in the Earth's crust (15–25 km) in the absence of vertical conductive beds in the lithosphere; *d*, UDFFS with a conductive layer in the Earth's crust (15–25 km) in the absence of vertical conductive beds in the lithosphere and high-resistivity layer in the asthenosphere. The width of the vertical conductive layers is 2 to 3 km, and the electrical resistivity is 5 Ohm·m.

riod range $1 < T < 10{,}000$ s (Fig. 7*a*). If $\rho_{кор.} = 20$ Ohm·m and $\rho^{\perp}$ increases, the shunting effect of the crustal conductive plate forms a clearly manifested minimum, which is replaced by an ascending branch at periods above 100 s (Fig. 7*b*). In both models, transverse curves outside of the UDFFS in the lithospheric blocks 1 and 2 in a period range $100 < T < 10{,}000$ s are represented by descending branches, which match the descending branches on the longitudinal curves $\rho^{//}$ in periods $T > 1000$ s. Over the entire profile in the lithospheric blocks 1 and 2, curves $\rho^{\perp}$ remain virtually the same. It is shown by a detailed analysis of the results that, in models *A* and *B*, the transition bands in which the transverse curves transform from "normal" to "anomalous" are several kilometers in length. The low-resistivity crustal plate is reflected on the transverse curves $\rho^{\perp}$ as a minimum. At the same time, the minimum on $\rho^{\perp}$ is noticeably shifted toward long periods relative to the corresponding minimum on curve $\rho^{//}$. The position of the minimum on $\rho^{\perp}$ is strictly related to the parameters of the conductive plate (the depth of occurrence and the electrical resistivity), which increases the possibility of interpreting the data.

The absence of translithospheric electrically conductive vertical zones in the tectonosphere section significantly affects the behavior of $\rho^{\perp}$, which becomes weakly sensitive to the presence of a horizontal conductive plate in the Earth's crust: instead of a clear minimum, there is a slight bend in an interval of 20–40 s (Fig. 7*c*). In a long-period range $T > 100$ s, curves $\rho^{\perp}$ slightly change their shape throughout the entire profile, representing a straightened line stretching to $T > 10\,000$ s. These curves can be used to establish the position of the projection of a high-resistivity asthenospheric insert on the day surface. The level of conformal shift of $\rho^{\perp}$ is determined by the resistivity of the near-surface layer of the sedimentary sequence.

If the tectonospheric section has no high-resistivity insert separating the conductivity of the asthenosphere, then the transverse curves $\rho^{\perp}$ virtually lose their sensitivity to conductive plates in the Earth's crust (Fig. 7*d*). Their shape is now determined by the parameters of the main horizontal layers of the tectonosphere and varies slightly along the profile. The apparent resistivity level at each particular observation point varies following the values of the electrical resistivity of the surface layer of the sedimentary stratum. Far from the near-surface heterogeneity (points 1 and 4), curves $\rho^{\perp}$ occupy their "true" level. In this case, the long-period falling branches $\rho^{\perp}$ match those on $\rho^{//}$, and the difference in the shapes of $\rho^{\perp}$ and $\rho^{//}$ in a period range $10 < T < 1000$ s is determined by their different sensitivity to the presence of linear conductors in the section.

Similar phenomena in the transformed MTS curves were obtained previously on the basis of modeling the geoelectric section of the tectonosphere using the AA′ profile along the shore line of the northern closure of the Gulf of Tonkin, where the presence of two UDFFSs of the southeastern strikes was recorded (Nikiforov et al., 2014, 2016, 2018). One of them gravitated toward the Red River fault zone, and the other toward the Cao Bang – Tien Yen Fault zone.

Thus, the mechanism of the monotonous growth of apparent resistivity with increasing periods up to 20,000 s, caused by the presence of an UDFFS structure in the section of the tectonosphere, is convincingly substantiated. By introducing vertical and horizontal electrically conductive bodies into various parts of the model and changing their parameters, one can obtain the whole variety of the shapes of MTS curves, characteristic of experimental data. In this case, the presence of low-resistivity (fluid-saturated) faults in the section, which extend to the base of the sedimentary sequence, is marked by a sharp change in the shape of the transverse curves $\rho^{\perp}$. This approach is used to zone the tectonosphere of North Vietnam with allocation of three UDFFSs (Fig. 8).

The role of a practical criterion for geoelectric zoning is played by the change of descending branches ρ^{*}_{xy} to ascending branches in a period range $T > 1000$ s, so it is not difficult to distinguish boundary 2 identified with the extension of the low-resistivity (fluid-saturated) conductor (fault) to the base of the sedimentary cover, which provides galvanic bonding of between the rocks of the sedimentary cover with electrically conductive asthenosphere (Fig. 8). To the north of boundary 2 at points NGL, YNB, TNQ, and TRS, curves ρ^{*}_{xy} are represented by descending branches at $T > 1000$ s. At the points located to the south of this boundary, curves ρ^{*}_{xy} have branches ascending in a range $10 < T < 2000$ s (HLG, CTB, and THB) or ascending branches complicated by a minimum. Further south, at points COT, COT2, NGV, and NIC, one may again observe curves ρ^{*}_{xy}, represented by a descending branch at $T > 1000$ s. The position of these points allows for a southern boundary denoting a change in the types of curves (boundary 1 in Fig. 8) to be drawn in the form of echelon-joined segments. Thus, between boundaries 1 and 2, there is a zone of anomalous behavior of ρ^{*}_{xy} in the long-period range, associated with the presence of high-resistivity disturbance I in the electrically conductive asthenosphere, and the axis of this zone extends in the northeast direction along the Kim Son – Lang Son line. The tectonic elements 1, I, and 2, which determine the anomalous behavior of ρ^{*}_{xy}, form the UDFFS of the northeastern strike.

The analysis of the apparent resistivity in the northeastern direction allows one to distinguish two abnormal zones of ρ^{*}_{yx}, associated with the presence of high-resistivity displacements with a southeastern strike in the asthenosphere.

The first zone (Fig. 8, elements 3, II, and 4) is substantiated by observations of MTS at points CTH, NIC, BOR, and THB. These points are located to the south of the high-resistivity asthenospheric displacement I (Kim Son – Lang Son). At points PYN and PTO, located north of displacement I, the ascending branches on curves ρ^{*}_{yx} are not shown. The considered behavior of ρ^{*}_{yx} in the western part of the investigated territory suggests that the high-resistivity lithospheric displacement II accompanying the Red River fault system, is developed only in the southern part of the region under

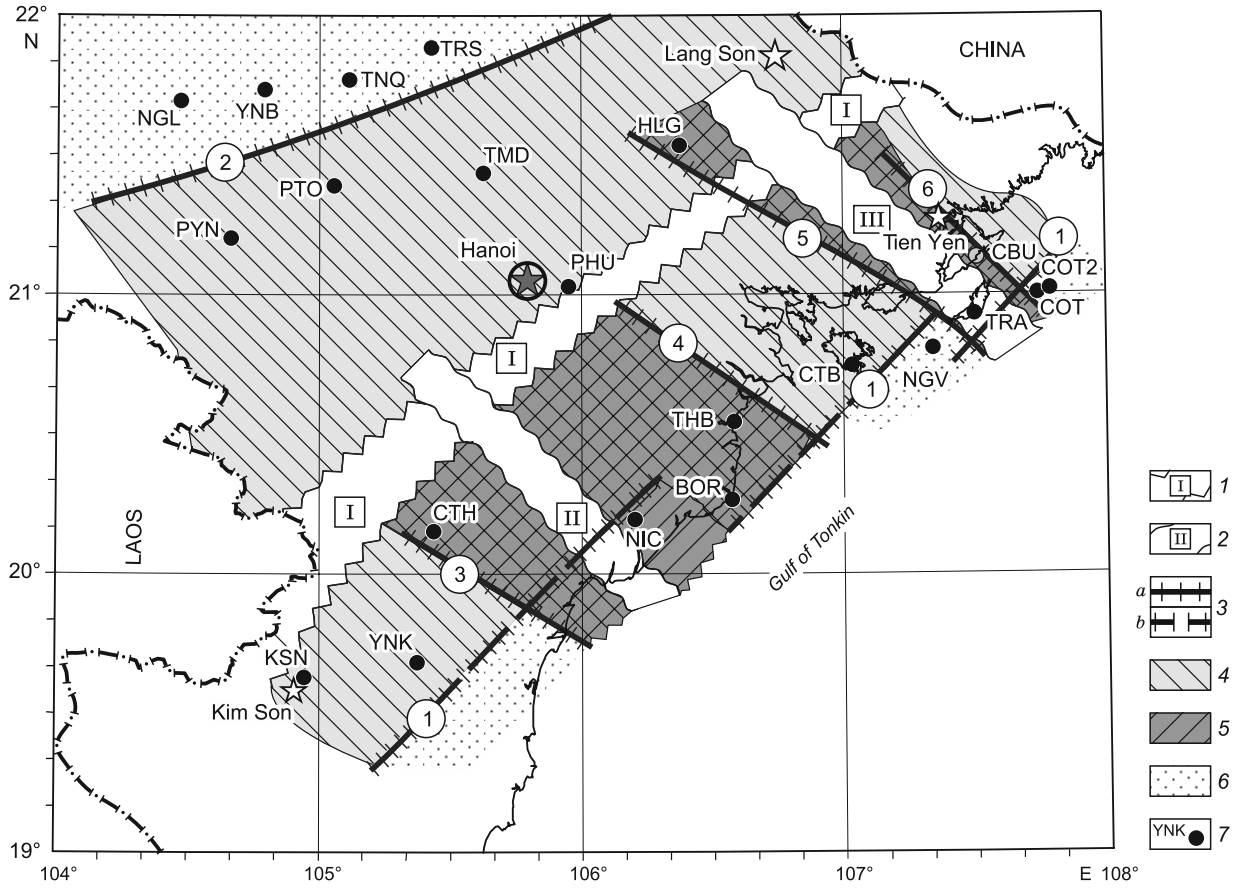

Fig. 8. Positions of the projections of UDFFSs of the tectonosphere of North Vietnam. *1,* projection onto the day surface of the high-resistivity disturbance system in the asthenosphere of the Kim Son – Lang Son northeastern strike (I); *2*, projection of the high-resistivity disturbance systems in the asthenosphere of the southeastern strike: II, system of the Red River fault zone, III, Tien Yen–Cao Bang system; *3*, extensions of the high-resistivity (fluid-saturated) translithospheric subvertical faults: *a*, determined, *b*, assumed; *4*, UDFFS of the northeastern strike; *5*, UDFFS of the southeastern strike; *6*, territories with normal apparent resistivity; *7*, MTS points and their names. The numbers in the circles denote the extensions of the high-resistivity translithospheric faults.

study and, probably, under the water area of the Gulf of Tonkin. It decays rapidly in the continental part in the northwest direction after crossing the Kim Son – Lang Son line. On both sides, the considered high-resistivity displacement is enclosed by low-resistivity translithospheric conductive layers (fault zones) 3 and 4 (Fig. 8).

The second zone (Fig. 8, elements 5, III, and b), which is associated with the high-resistivity lithospheric displacement III, is determined by data at HLG, CBU, and TRA in the eastern part of the area under study. Displacement III crosses the Kim Son – Lang Son line, but it is unknown at this stage of investigation whether it decays immediately after the crossing or extends far in the northern-western direction. On the territory under study, it is bounded on both sides by low-resistivity translithospheric faults 5 and 6. The position of the latter is shown conditionally as the boundary at which the type of curves ρ^*_{yx} changes is marked at one COT point.

The combined analysis of curves ρ^*_{xy} and ρ^*_{yx} allows one to obtain an idea of the skeleton frame of the geoelectric depth model of North Vietnam. It is shown by ultradeep fluid-fault steeply dipping systems intersecting virtually orthogonally and developed in a layered section. A more detailed analysis of the apparent resistivity, specifically complications on the ascending branches of curves $\rho_к$, yields a certain idea about the spatial location of electrically conductive formations in the crust and subcrustal lithosphere.

In the family of curves ρ^*_{xy} (apparent resistivity in the northern-western direction) has a large group characteristic for the presence of a minimum in a range $50 < T < 500$ s, preceding the ascending branch at $T > 1000$ s. According to numerical modeling of the geoelectric section, this nature of ρ^*_{xy} is due to the presence of plates at different deep intervals. The modeling of the position of these minima on a period axis, their width, and the position of apparent resistivity on the axis can help one obtain an idea about the deep intervals of development of low-resistivity formations (Fig. 9*c*). If the values of electrical resistivity lies in a range $10 < \rho < 20$ Ohm·m, the experimental curves ρ^*_{xy} match model curves by their shape the best. As seen from the section of profile

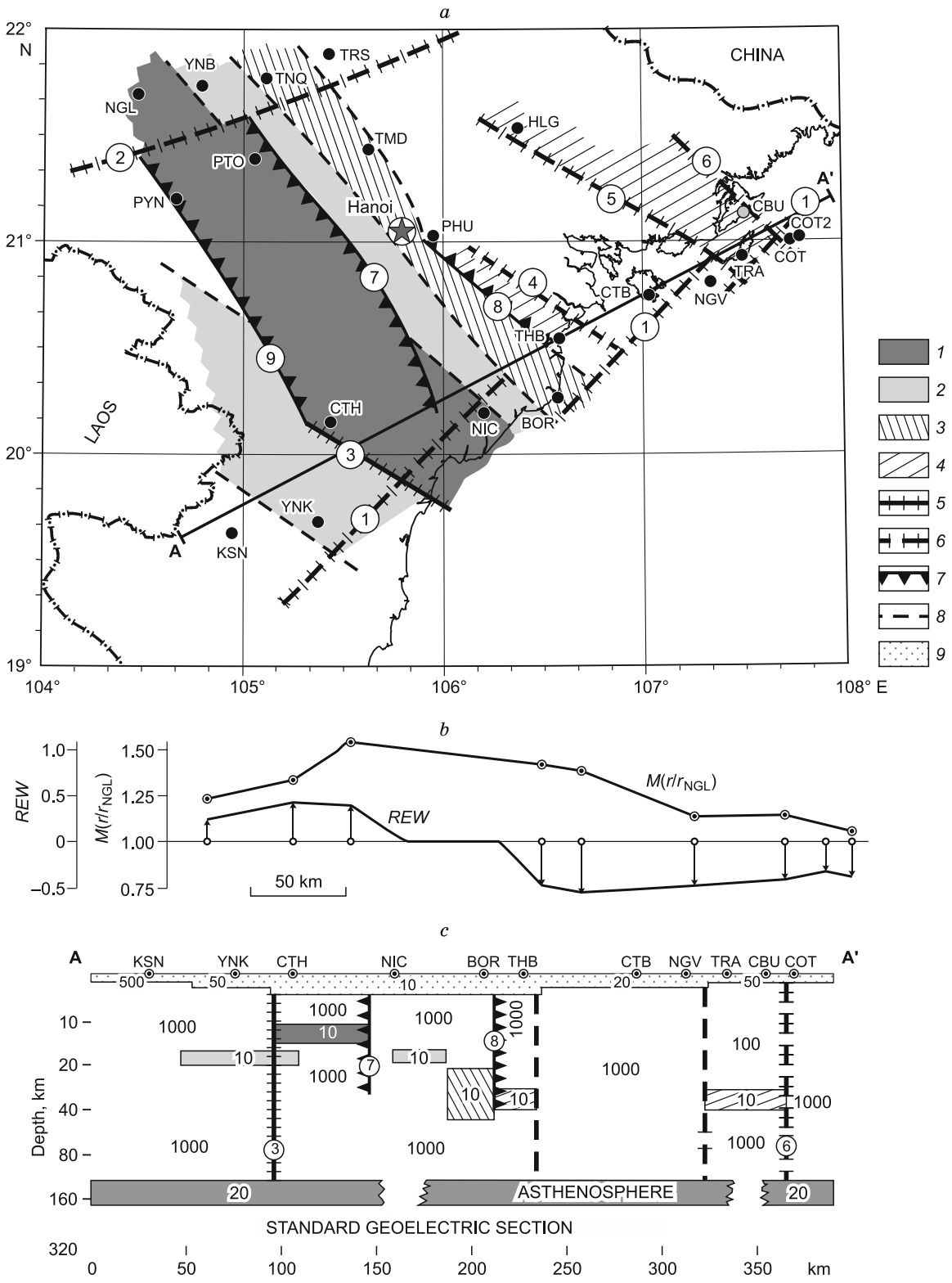

Fig. 9. Geoelectric model of the tectonosphere of North Vietnam. *a*, diagram of electrical conductivity; *b*, chart for tippers (*REW*) and horizontal magnetic responses ($M\ (r/r_{NGL})$); *c*, geoelectric section of the tectonosphere along profile A–A′. *1*, *2*, low-resistivity rocks in the upper, middle, and lower parts of the Earth's crust; *3*, anisotropic-conductive rocks in the middle part of the lithosphere; *4*, anisotropic-conductive rocks near the Moho discontinuity; *5*, translithospheric solid low-resistivity faults; *6*, translithospheric discrete low-resistivity faults; *7*, crustasl low-resistivity faults; *8*, projections of the conductivity boundaries in the lithosphere; *9,* sedimentary cover rocks. The numbers in the circles denote faults, and the numbers in section *c* denote the resistivities of the block rocks (Ohm·m).

A–A′ (Kim Son – Co To), the conductive crustal formations are maximally close to the day surface at a depth of 10 km in the vicinity of points CTH and NIC. Geographically, this zone of elevation of crustal conductive formations extends in the northwest direction and is clearly fixed in the north of the region at points PYN and PTO (Fig. 9*a*). Tectonically, it corresponds to the fault system of the Da River. This electrically conductive crustal zone plunges in the northeast direction to a roof depth of up to 20 km. Judging by the fact that, at points BOR and TMD, cortical conductivity is observed only for the northwest direction and is not fixed in the orthogonal direction, we can assume that the band with the TNQ, TMD, and BOR axial line in the middle part of the lithosphere (20–50 km) has a system of close low-resistivity faults of the northwestern direction, which match the fault zone of the Red River. It is interesting to note that, at point TNQ located outside the anomalous zone of the UDFFS of the Kim Son – Lang Son line, a crustal conductor is presented differently than inside the UDFFS itself, which fits well with the modeling results. At this point, the crustal conductor is marked on ρ^*_{xy} as a minimum against the background of a general decrease in the apparent resistivity.

To the west of the fault system of the Da River, a possibly separate, electrically conductive crustal zone is located in a depth interval of 15–25 km. It is well manifested on curves ρ^*_{xy} at points YNK and CTH. Based on the azimuthal analysis, we can confidently state that the *X* axis at these points has a direction of 310–320°, which contrasts with a value of 325–335° observed at all other points. In addition, as shown in Fig. 2, this zone associated with the fault system of the Ma River, steadily turns the tipper arrow at PYN closer to the north at all periods.

The change in the apparent resistivity ρ^*_{yx} in the northeast direction indicates that the geoelectric model has several zones that are electrically conductive (anisotropic) in the northeast direction. Their peculiarity lies in the fact that they have a northwestern strike that is orthogonal to conductivity. As is known (Berdichevskii et al., 1991; Berdichevskii, 2010), the reflection of the core conductor on curves orthogonal to the strike of the zones is possible if it has a galvanic coupling with the sedimentary sequence. Given this property of the MTS curves, the model is supplemented with the low-resistivity faults 7, 8, and 9, penetrating to a depth of about 40 km and providing the indicated relationship (see Fig. 9*a*, *b*).

The zone bounded by faults 7 and 9 at points PYN, PTO, and CTH contains conductive crustal formations, which appear on the mutually perpendicular curves ρ^*_{yx} and ρ^*_{xy} simultaneously and in different ways. It can be assumed that this is the way that an isotropically conductive crustal plate is reflected on the MTS curves, which, according to the numerical simulation estimates, lies at a depth interval of 10–15 km. At points NGL (to the north of fault line 2) and NIC (south of fault line 1), curves ρ^*_{yx} orthogonal to the strike of the zone show no complications indicating the presence of a crustal conductor. This is probably due to the absence of low-resistivity faults in these parts of the section, providing galvanic coupling between the crust conductor under consideration and the sedimentary sequence. For this reason, it is shown only on curves ρ_{xy}.

In the zones between faults 8–4 and 5–6, the crustal low-resistivity conductors are fixed only on curves ρ^*_{yx}, orthogonal to the strike. According to calculations, these anisotropic-conductive formations are widespread in a depth interval of 30–40 km, i.e., they are located near the Moho discontinuity (Nikiforov et al., 2014, 2018).

It is shown by the analysis of magnetic responses (Figs. 2, 3*a*, *b*, and 9*b*) that they are mainly associated with elements of the geoelectric depth model and extend in the northwest direction. These include the translithospheric fault 3, the crustal faults 7, 8, and 9, and the crustal electrically conductive systems of the Ma, Da, and Red rivers (Fig. 10).

The most elevated crustal electrically conductive system of the Da River (the depth of the top edge is about 10 km) along with the listed low-resistivity faults extending into the base of the sedimentary sequence (at a depth of not more than 2 km) form a zone of minimum values for the tipper and maximum values for the horizontal magnetic response $M\left(r/r_{\mathrm{NGL}}\right)$ or $M\left(r/r_{\mathrm{CTB}}\right)$ on the day surface. The boundaries of the zones of the crustal electrically conductive systems along with the low-resistivity faults are located in the model with maximum agreement in terms of the large axes of the ellipses $M\left(r/r_{\mathrm{CTB}}\right)$ (Fig. 10).

To the northeast of this conductive system that is as close as possible to the surface, the REW tippers are aligned in northeast azimuths. Their weak decay is due to the presence of another more submerged crustal electrically conductive system of the Red River, located hypsometrically below the crustal system of the Da River. As the electrically conductive system of the Red River is maximally manifested in a depth range of 20–50 km, it has little effect on the character of ellipses $W\left(r/r_{\mathrm{CTB}}\right)$ and the appointment of the REW tippers directly above the system.

To the southwest of the translithospheric fault 3, which bounds the conductive system of the Da River, the electrically conductive crustal system of the Ma River is located hypsometrically lower (15–20 km). It is slightly more turned westwards. With this azimuthal unconformity with the Da system, there is an obvious change in the direction of the tippers at point PYN and on the large axes of the ellipses $W\left(r/r_{\mathrm{CTB}}\right)$ at points KSN and YNK.

At this stage of the study, the magnetic responses of the medium seem to have no pronounced relationship with faults 1 and 2 of the northeastern direction and faults 8, 4, 5, and 6 of the northwestern direction. The listed faults are the main elements of the geoelectric depth model, which are associated with characteristic of apparent resistivity. Considering that the vertical conductivity of faults is important for the formation of apparent resistivity anomalies and their horizontal conductivity is important for the formation of

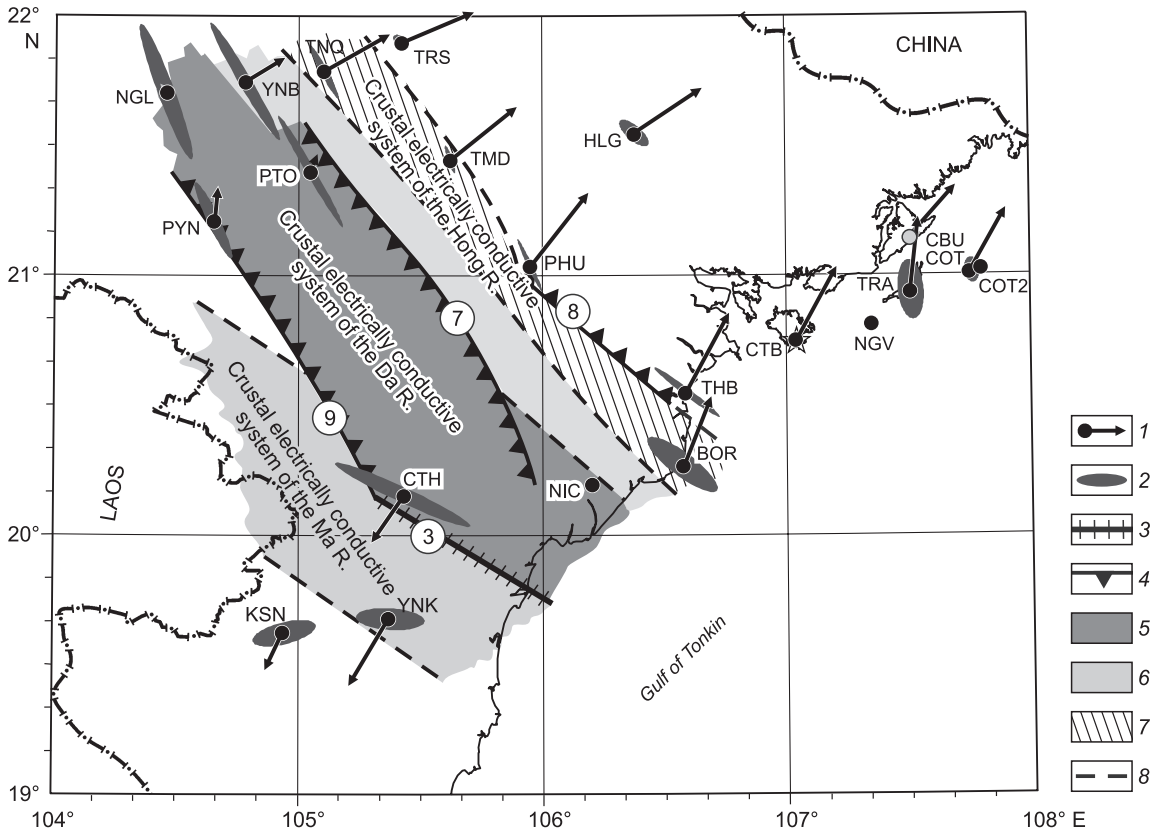

Fig. 10. Elements of the geoelectric model of the tectonosphere that determine the magnetic responses of the medium. *1*, tippers; *2*, ellipses of horizontal responses relative to point CTB; *3*, low-resistivity (fluid-saturated) translithospheric faults; *4*, low-resistivity (fluid-saturated) crustal faults; *5*, *6*, low-resistivity plates in the Earth's crust: *5*, a depth interval of 10–15 km, *6*, a depth interval of 15–20 km; *7*, zone with formations that are anisotropic-conductive in the northwestern direction in a depth interval of 20–40 km; *8*, projection of the boundaries of the crustal longitudinal bodies onto the surface. The numbers in the circles indicate the low-resistivity faults that extend to the surface.

magnetic anomalies, we can assume that these faults are not solid bodies capable of electrical conduction in horizontal directions.

RESULTS AND DISCUSSION

Long-period electromagnetic studies ($10 < T < 20{,}000$ s) performed according to the programs of Russian-Vietnamese scientific cooperation on the territory of North Vietnam contributes to obtaining new results both in the field of electromagnetic phenomena in the heterogeneously conducting section of the tectonosphere and in the field of developing new ideas about a deep-seated structure in the junction zone of the Indochina and South China geoblocks. As it turns out, the most important feature of a long-period electromagnetic process is the galvanic interaction of deep-seated electrically conductive systems (conductive asthenosphere and subasthenospheric horizons) with the conductive system of a sedimentary cover, including the water layer. Interaction occurs via subvertical (steeply dipping) electric current conductors associated with the fluid system of discontinuous and fracture displacements, which form through translithospheric faults.

In the superposition zone of near-surface and deep-seated currents differing in their frequency characteristics, there are generated anomalous apparent resistivity curves whose mandatory component is the ascending branch at $T > 1000$ s. The individual features of the anomalous MTS curves are also determined by the presence of conductive bodies in the geoelectric section of the lithosphere, which are adjacent to conductive subvertical faults (channels), and by the heterogeneous electrical resistivity of the surface layer in which telluric currents are recorded. In this regard, separating local and regional magnetotelluric effects is especially important for data interpretation. The above-given approaches for solving this problem allow one to obtain initial impedance responses (almost inconsistent among themselves) to a system with stably expressed patterns of variation over the area under study.

The main elements of the model are multidirectional vertical electrically conductive plates identified with fluid-saturated faults of various ranks and dividing the layered section of the tectonosphere (very similar in parameters to the section of Sakhalin, Kamchatka, and Japan) into geoblocks of various scales.

Anomalous vertical and horizontal magnetic fields have a simple structure generally matching a corresponding two-dimensional model. In this case, the position of the crustal conductive bodies of the northwestern strike in the Ma – Red – Lo rivers interfluve, identified by interpreting the apparent resistivity, satisfies the character of the REW tippers and ellipses $M\left(r/r_{\text{CTB}}\right)$. At the same time, magnetic anomalies react weakly to a number of conductive bodies in the lithosphere of both northwestern and northeastern strikes. This leads to the conclusion that fault zones can have both vertical and horizontal conductivity in some cases and only vertical conductivity in other cases. The fact that electric and magnetic fields respond to the elements of the geoelectric structural tectonosphere in different ways makes it important to integrate MTS and MVS. It allows one to obtain a more complete pattern of the deep-seated structure, which cannot be done by each method separately.

The position of the main faults of the region relative to the elements of the proposed geoelectric model of the tectonosphere is shown in Fig. 11. It can be seen that the faults of the Red, Chay, and Lo rivers match the projections onto the day surface of the boundaries of conductive prisms in the Earth's crust. They are also in good agreement with how the fragments of the fluid-saturated faults 3, 7, 8, and 9 extend to the base of the sedimentary sequence (Fig. 9). As noted above, these elements of the model create anomalies in the magnetic field.

Figure 11 also shows the location of ore, naphthide, and hydrothermal deposits in the geoelectric structure of the region. It is clearly seen here that the location of the deposits is controlled by the exit lines of vertical electrically conductive faults of a predominantly northeastern direction (fault zones 1 and 2). Moreover, most deposits are located near the intersection of displacements 1 and 2 with displacements of the northwestern direction. It can also be noted that oil and gas deposits near the Red River and asphalt deposits on the Cat Ba Island and near the Yen Bai City are associated with extensions to the base of the sedimentary sequence of electrically conductive translithospheric faults. Apparently, this is characteristic for the entire junction zone of the Asian continent with marginal seas. In the oil and gas basins of Sakhalin, the exact same pattern of location of hydrocarbon deposits of the relative geoelectric structure is found (Nikiforov et al., 2016)

The relation between geological objects and phenomena with the geoelectrical structure elements indicates that geological processes are accompanied by changes in the electrical resistivity of adjacent strata. Dry rocks are characterized by a high resistivity of 104–106 Ohm·m. Under the influence of temperature and pressure, it monotonically de-

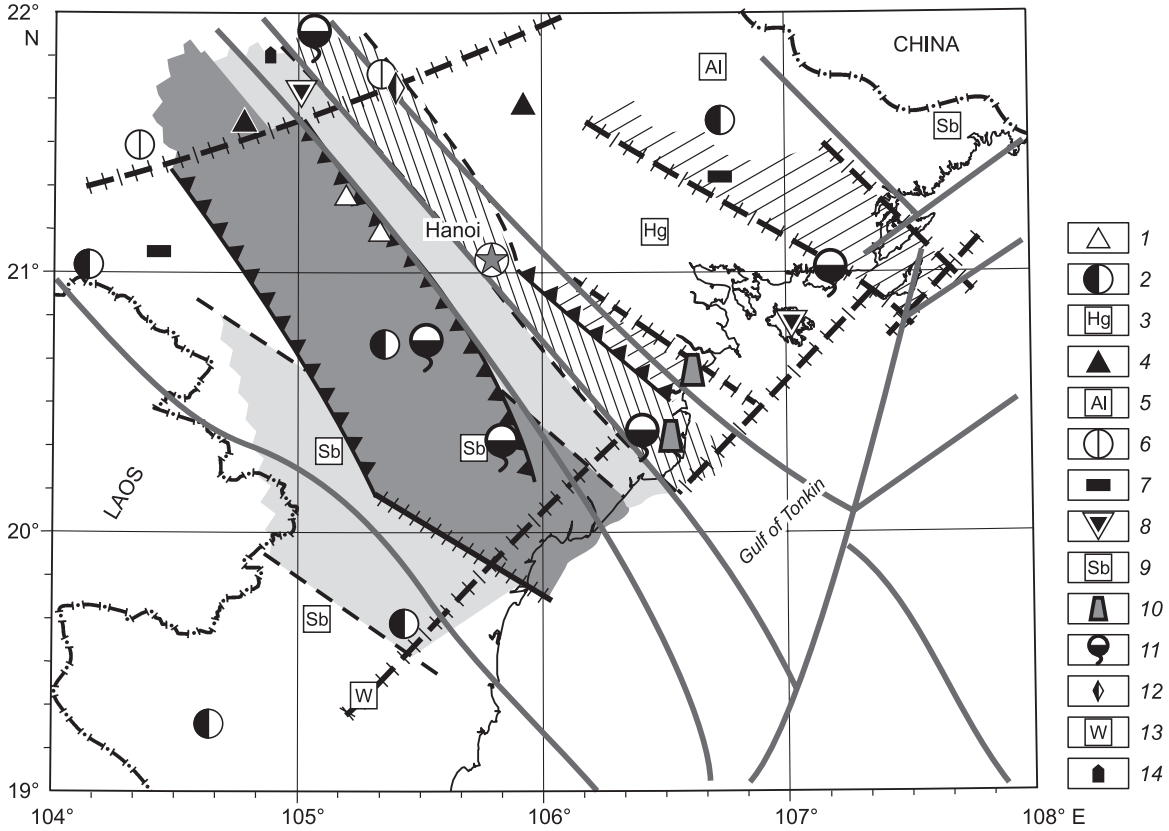

Fig. 11. Relation between the geoelectric structure and the location of minerals and the main faults of North Vietnam. Minerals: *1*, pyrite; *2*, gold; *3*, mercury; *4*, iron; *5*, aluminum; *6,* Pb–Zn ore; *7*, copper ore; *8*, asphalts; *9*, antimony; *10*, gas field, *11*, hydrothermal springs, *12*, titanium, *13*, tungsten, *14*, granite. The remaining denotations are in Figs. 1, 9 and 10.

creases over depth. The nature of highly conductive horizons is considered in detail in (Kissin, 1994; Van'yan, 1997). It is associated in most models mainly with the partial melting of the upper mantle substance and the dehydration of the crustal substance under certain conditions. Insufficient attention has been paid to the study of deep-seated vertical geoelectric structures. In (Nikiforov et al., 2013, 2016, 2018), the deep degassing of the Earth is considered to be one of the possible reasons for the presence of vertical geoelectric structures in the tectonosphere. The main components of the deep fluid are considered to be the H_2, CO_2, CO, C H_4, and H_2O gases (Kadik and Lukanin, 1986). Depending on their quantitative ratio, temperature, pressure, stress-strain state, the petrological properties of the host rocks, etc., the fluid state transforms. Usually, several types of reactions in the Earth's crust and the upper mantle are considered, which result in the formation of an electrically conductive material (Kadik and Lukanin, 1986):

$2CO \Leftrightarrow C_{(graphite)} + CO_2$,

$CO_2 + 2H_2 \Leftrightarrow C_{(graphite)} + 2H_2O$,

$CO + H_2 \Leftrightarrow C_{(graphite)} + H_2O$,

$CO_2 + CH_4 \Leftrightarrow 2C_{(graphite)} + 2H_2O$,

$15FeO + CO_2 \Leftrightarrow Fe_3C_{(cohenite)} + 5Fe_2O_3 + 2FeO$,

$Fe_3C + 2O_2 \Leftrightarrow Fe_3O_4 + C$.

During deep fluid pumping, the multiscale cracks, which form a fault zone along which the mantle substance is transferred to the upper layers of the Earth's crust, are filled with an electrically conductive material that is the product of the above-given reactions. Conductive bodies become "visible" for deep electrical exploration methods. The search for vertical conductive zones is important for solving fundamental and applied problems. Typically, linear electrically conductive bodies in the lithosphere create longitudinal apparent resistivity anomalies and magnetic response anomalies. Their interpretation has a well-known drawback: contiguous electrically conductive bodies are reflected as a whole. But, despite this, anomalously conducting zones are actively studied on all continents in the most diverse tectonic situations, even in an integral representation. They are associated with deposits of diamonds, ores, hydrocarbons, thermal springs, seismically active lineaments, etc.

During the fault zone evolution, a fusible material can be carried out in large quantities into the upper layers and refractory restite can deposit through it (Bogatikova et al., 1988). If the latter accumulates in quantities sufficient for the formation of a barrier that poorly conducts electric current and divides the asthenosphere into separate blocks, then a geoelectric model arises (Fig. 7), discussed in detail above. Its peculiarity and uniqueness lies in the fact that it allows one to use the tracking of transverse apparent resistivity anomalies to reliably trace the extensions of deep-seated conductive (fluid-saturated) faults into the base of the sedimentary sequence, to estimate the depth of their penetration into the lithosphere, and to study the block structure of the lithosphere and crustal conductive plates in detail. This model explains the nature of the MT and MV anomalies of North Vietnam and provides a key to understanding the nature of the layered-block structure of the lithosphere. In particular, in the northwestern part of the area under study, according to (Dolginov et al., 2011), there is a "hot spot" in the tectonosphere at a depth of about 250 km, which is the melting zone of the upper mantle substance. For this reason, in the asthenosphere, the temperature conditions at the "hot spot" do not contribute to the accumulation of "hard" high-resistivity restites. The absence of a high-resistivity barrier in the asthenosphere in this section of the territory makes the transverse apparent resistivity curves uninformative. Thus, the MT and MV responses acquire properties characteristic of two-dimensional media.

CONCLUSIONS

1. The territory of North Vietnam is located at the intersection of orthogonal UDFFS of northeastern and southeastern strikes. Geoelectrically, these systems are represented by vertical high-resistivity displacements separating the electrically conductive asthenosphere and high-resistivity (2–5 Ohm×m) plates (fault zone), penetrating the entire lithosphere, and providing galvanic coupling between the conducting asthenosphere and sedimentary sequence.

2. Low-resistivity (fluid-saturated) translithospheric faults extending to the base of the sedimentary sequence and reliably fixed by the MTS method control the location of petroleum fields and ore deposits.

3. The presented structural features of the deep-seated section of the tectonosphere of North Vietnam explain why the impedance and magnetic responses of the electromagnetic field are formed by various elements of the geoelectric model in the area under study. Combining the MT and MV methods allows one to investigate the geoelectric structure of the area under study more profoundly.

4. The method is proposed for separating local and regional magnetotelluric effects, which makes it possible to reliably determine the main directions of the regionally two-dimensional structure and the configuration of the apparent resistivity curves in the main directions.

5. It is recommended to continue using the MT and MV methods to study the explosive fluid-saturated displacements revealed on land in the Gulf of Tonkin. Investigating them and the electrical parameters overlapping the Cenozoic sediments can become the basis for developing directions for continuing oil and gas exploration on the shelf of the region.

This work was financially supported within the framework of the "Dal'nii Vostok" program by the Far Eastern Branch of the Russian Academy of Sciences as part of the scientific projects VANT 19-021 and 18-1-004, the state budget issues 0271-2019-0002, 0144-2019-0021 and the VAST QTRU project 02.01/19-20

REFERENCES

Bahr, K. 1988. Interpretation of the magnetotelluric impedance tensor: regional induction and local telluric distortion. J. Geophys., 62, 119–127.

Berdichevskii, M.N., Dmitriev, V.I., 2010. Models and Methods of Magnetotellurics [in Russian]. Nauchnyi Mir, Moscow.

Berdichevskii, M.N., Dmitriev, V.I., Kulikov, V.A., 1991. Normalization of a Magnetotelluric field by fluid-saturated faults. Fizika Zemli, No. 3, 45–51.

Bogatikova, O.A., Laz'ko, E.E., Sharkova, E.V. (Eds.), 1988. Magmatic Rocks. Vol. 5. Ultrabasic Rocks [in Russian]. Nauka, Moscow.

Caldwell, G.T., Bibby, H.M., Brown, C., 2004. The magnetotelluric phase tensor. Geophys. J. Int. 158, 457–469.

Dinh, V.T., Harder, S., Huang, B.S., Trinh, V.B., Doan, V.T., Lai, H.P., Tran, A.V., Nguyen, H.Q., Nguyen, V.D., 2018. An overview of northern Vietnam deep crustal structures from integrated geophysical observations. Terr. Atmos. Oceanic Sci. 29 (4), 371–386.

Doan, T.V., Dinh, T.V., Nguyen, Y.T., 2001. Deep structure feature of the Red River fault zone and its geodynamic implication from magnetotelluric data. Tạp chí Địa chất (Vietnam J. Geol.), A 267, 21–28 [in Vietnamese with English Abstract].

Dolginov, E.A., Kao, T.D., Le V.Z., Ngo, T.L., Bashkin, Yu.V., 2011. On the possible deep nature of the seismic anomaly in North-West Vietnam and its relationship with a reactivated "hot spot" system of the of the Late Jurassic – Early Cretaceous periods. Izvestiya Vuzov. Geologiya i Razvedka, No. 2, 11–16.

Groom, R.W., Bailey, R.C., 1989. Decomposition of magnetotelluric impedance tensors in the presence of local three dimensional galvanic distortion. J. Geophys. Res. 94, 1913–1925.

Kadik, A.A., Lukanin, O.A., 1986. Upper Mantle Degassing During Melting [in Russian]. Nauka, Moscow.

Kissin, I.G., 1994. Fluid Saturation of the Crust, electrical conductivity, and seismicity. Fizika Zemli, No. 4, 30–40.

Korepanov, V., Klymovych, Y., Kuznetsov, O., Pristay, A., Marusenkov, A., Rasson, J., 2007. New INTERMAGNET fluxgate magnetometer. Publs. Inst. Geophys. Pol. Acad. Sc., C-99 (398), 291–298.

Kuznetsov, V.A., 2005. Normalization of the MT curves distorted by the S-effect. Fizika Zemli, No. 7, 91–96.

Minh, L.H., Toan, D.V., Son, V.T., Thang, N.C., Duan, N.B., Thanh, N.H., Thanh, L.T., Marquis G., 2011. Preliminary results of processing the sounding magnetotelluric data of Hoa Binh-Thai Nguyen and Thanh Hoa-Ha Tay profiles. Tạp chí Các Khoa Học Về Trái Đất (Vietnam J. Earth Sci.), 33 (1), 18–28 [in Vietnamese with English Abstract].

Moroz, Yu.F., 1991. Electrical conductivity of the Earth's crust and the upper mantle of Kamchatka [in Russian]. Nauka, Moscow.

Nielsen, L.H., Mathiesen, A., Bidstrup, T., Vejbek, O.V., Dien, P.T., Tiem, P.V., 1999. Modelling of hydrocarbon generation in the Cenozoic Song Hong Basin, Vietnam: a highly prospective basin. J. Asian Earth Sci. 17, 269–294.

Nikiforov, V.M., Dolgikh, G.I., Kulinich, R.G., Shkabarnya, G.N., Dmitriev, I.V., Phung Van Phach, Hoang Van Vuong., 2014. New data on the deep structure of the northern part of the Gulf of Tonkin in the South China Sea based on the results of magnetotelluric soundings. Dokl. Earth Sci. 458 (2), 1302–1306.

Nikiforov, V.M., Kulinich, R.G., Valitov, M.G., Dmitriev, I.V., Starzhinsky, S.S., Shkabarnya, G.N., 2013. Peculiarities of the fluid regime in the lithosphere of the junction zone between South Primorye and the Sea of Japan from the comprehensive geophysical data. Russ. J. Pac. Geol. 7, 46–55.

Nikiforov, V.M., Pal'shin N.A., Starzhinsky, S.S., 2004. Numerical modeling of the three-dimensional coastal effect in the Primorski region. Izv. Phys. Solid Earth 40 (8), 660–671.

Nikiforov, V.M., Shkabarnya, G.N., Kaplun, V.B., Zhukovin, A.Yu., Varentsov, I.M., Palshin, N.A., Cuong, D.H., Trung, N.N., Hung, D.Q., 2018. Electroconducting elements of the ultradeep fluid–fault systems as indicators of seismically active zones of the Eastern Margin of the Eurasian continent: evidence from magnetotelluric data. Dokl. Earth Sci. 480, 831–838.

Nikiforov, V.M., Shkabarnya, G.N., Zhukovin, A.Yu., Kaplun, V.B., Palshin, N.A., Varentsov, I.M., Do Huy Cuong, Phung Van Phach, Hoang Van Vuong, Starzhinsky, S.S., 2016. Vertical fault systems in the tectonosphere geoelectrical section in petroliferous domains of Sakhalin Island (Russia) and Gulf of Tonkin (Vietnam): Evidence from magnetotelluric sounding. Russ. J. Pac. Geol. 10, 395–407.

Phach, P.V., 2001. Tectonic structure of the Red River fault zone. Vietnam J. Geol., Series B 17–18, 1–11. (available in English on https://www.researchgate.net/publication/315316574_TECTONIC_STRUCTURE_OF_THE_RED_RIVER_FAULT_ZONE)

Phuong, N.H., 1991. Probabilistic assessment of earthquake hazard in Vietnam based on seismotectonic regionalization. Tectonophysics 198 (1), 81–93.

Pospeeva, E.V., 2008. Application of medium-scale magnetotelluric sounding to identify deep criteria for promising areas for kimberlite exploration. Russ. J. Pac. Geol. 27 (3), 18–32.

Utada, H., Baba, K., 2014. Estimating the electrical conductivity of the melt phase of a partially molten asthenosphere from seafloor magnetotelluric sounding data. Phys. Earth Planet. Int. 227, 41–47.

Van'yan, L.L., 1997. Electromagnetic Sounding. Nauchnyi Mir, Moscow.

Van'yan, L.L., Egorov, I.V., Shilovskii, A.P. 1986. Magnetotelluric excitation of extended conductive zones of the Earth's crust and asthenosphere. Fizika Zemli, No. 6, 70–76.

Varentsov, I.M., 2002. A general approach to the magnetotelluric data inversion in a piecewise-continuous medium. Izv. Phys. Solid Earth 38 (11), 913–934.

Varentsov, I.M., 2015. Arrays of simultaneous electromagnetic soundings: design, data processing, analysis, and inversion, in: Spichak, V. (Ed.), Electromagnetic Sounding of the Earth's Interior: Theory, Modeling, Practice. Elsevier, Amsterdam.

Varentsov, I.M. 2016. New algorithms in the software system for processing data of synchronous MT/MV soundings. Voprosy Estestvoznania, No. 3 (11), 48–52.

Varentsov, I.M., Sokolova, E.Yu., Martanus, E.R., Nalivaiko, K.V., 2003. System of electromagnetic field transfer operators for the BEAR array of simultaneous soundings: methods and results. Izv. Phys. Solid Earth, 39 (2), 118–148.

Editorial responsibility: A.D. Duchkov